

the EEO expressed the epithelial marker CDH1 (cadherin 1 or E-cadherin). After 5–10 d of culture, the organoids could be dissociated into mainly single cells that would regenerate and form organoids that could be achieved for more than 15 passages. A cryopreservation protocol was established for long-term storage of the organoids that allowed them to be thawed, regrown, and expanded (*Materials and Methods* and *SI Appendix, Fig. S1*).

EEO Exhibit Physiological Hormone Responsiveness. The human endometrium undergoes extensive remodeling during the menstrual cycle that is chiefly regulated by the ovarian steroid hormones E2 and P4 (14, 15). To investigate the hormone responsiveness of organoids in vitro, EEO were generated from endometrial biopsies of 2 different donors and then differentiated with either E2; E2 and medroxyprogesterone acetate (MPA), a nonmetabolizable form of progesterone; and E2+MPA+cAMP (cAMP) (Fig. 1A). Note that cAMP potentiates secretory transformation of human endometrial GE cells (11) and decidualization of endometrial stromal cells (16).

Forkhead box A2 (FOXA2) is a transcription factor that is expressed specifically in the GE of the endometrium of the human uterus (17). Consistent nuclear FOXA2 was observed in cells within the EEO (Fig. 1B). Not all cells within a single organoid were FOXA2 positive, and none of the treatments affected the number of FOXA2-positive cells in the EEO. The Ki67 proliferation marker was observed in cells of all EEO in every treatment group, and the number of Ki67⁺ cells increased with E2 treatment as compared to control untreated day 6 organoids (Fig. 1B). Similar to FOXA2, not all cells within a single organoid were Ki67 positive.

In day 6 EEO, treatment with E2 increased the number of E2 receptor (ESR1) and progesterone receptor (PGR)-positive cells compared to the control (Fig. 1C). In contrast, the number of ESR1 and PGR-positive cells was substantially lower in day 12 control and E2+MPA-treated organoids. The decrease and absence of PGR and ESR1 in the EEO with MPA treatment are consistent with the loss of PGR and ESR1 from the LE and GE that is observed in the endometrium between the proliferative to the secretory phase of the menstrual cycle (18).

Next, established E2- and P4-stimulated genes were measured in the EEO using real-time quantitative PCR (Fig. 2). In day 6 organoids, E2 treatment increased *OLFM4* and *IHH* mRNA levels in EEO from both donors. In day 12 organoids, an increase in expression of those genes was observed in the E2+MPA as compared to control organoids generated from Donor 2 but not Donor 1. With respect to P4-responsive genes, *HSD17B2*, *PAEP*, and *SPP1* were up-regulated by MPA treatment in day 12 organoids. Note the substantial increase in *HSD17B2* and *PAEP* mRNA levels in E2+MPA and E2+MPA+cAMP organoids as compared to day 12 control organoids. A small increase in these genes was observed in day 6 organoids treated with E2, but that increase was dependent on donor.

Transcriptomic Response of Organoids to Steroid Hormones. Bulk RNA-seq analysis of Donor 2 EEO revealed significant changes in gene expression depending on hormone treatment (Fig. 3A and *Dataset S1*). Treatment with E2 increased 1,093 genes and decreased 398 genes compared to control. The most increased gene was *OLFM4*, which is also increased during the proliferative phase of the menstrual cycle when E2 is the dominant

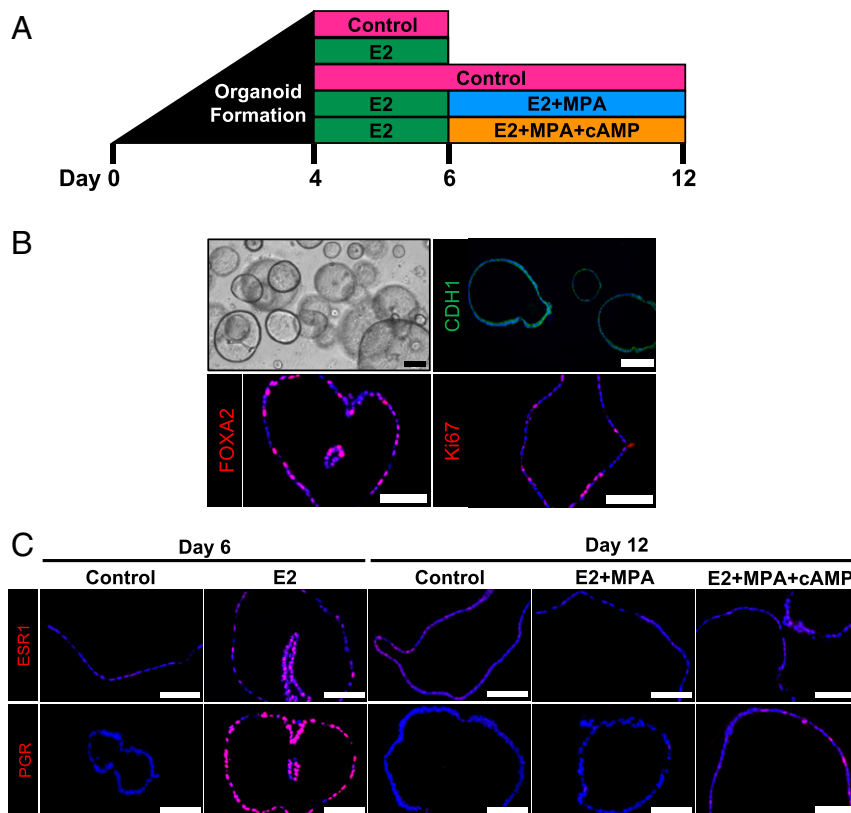


Fig. 1. Human endometrial epithelia organoids exhibit appropriate responses to ovarian steroid hormones. (A) Organoids were treated with either nothing (Control) or E2, followed by either nothing (control), E2+MPA, or E2+MPA+cAMP. (B) Round organoids formed under specific culture conditions as described in *Materials and Methods* and express CDH1, FOXA2, and Ki67. (C) ESR1 and PGR localization is increased in response to E2 which is seen in vivo. Organoids were counterstained with Hoechst (blue) to visualize nuclei. (Scale bars: *B* Upper Left, 200 μ m; *B* Upper Right, 100 μ m; *B* Lower and *C*, 75 μ m.)

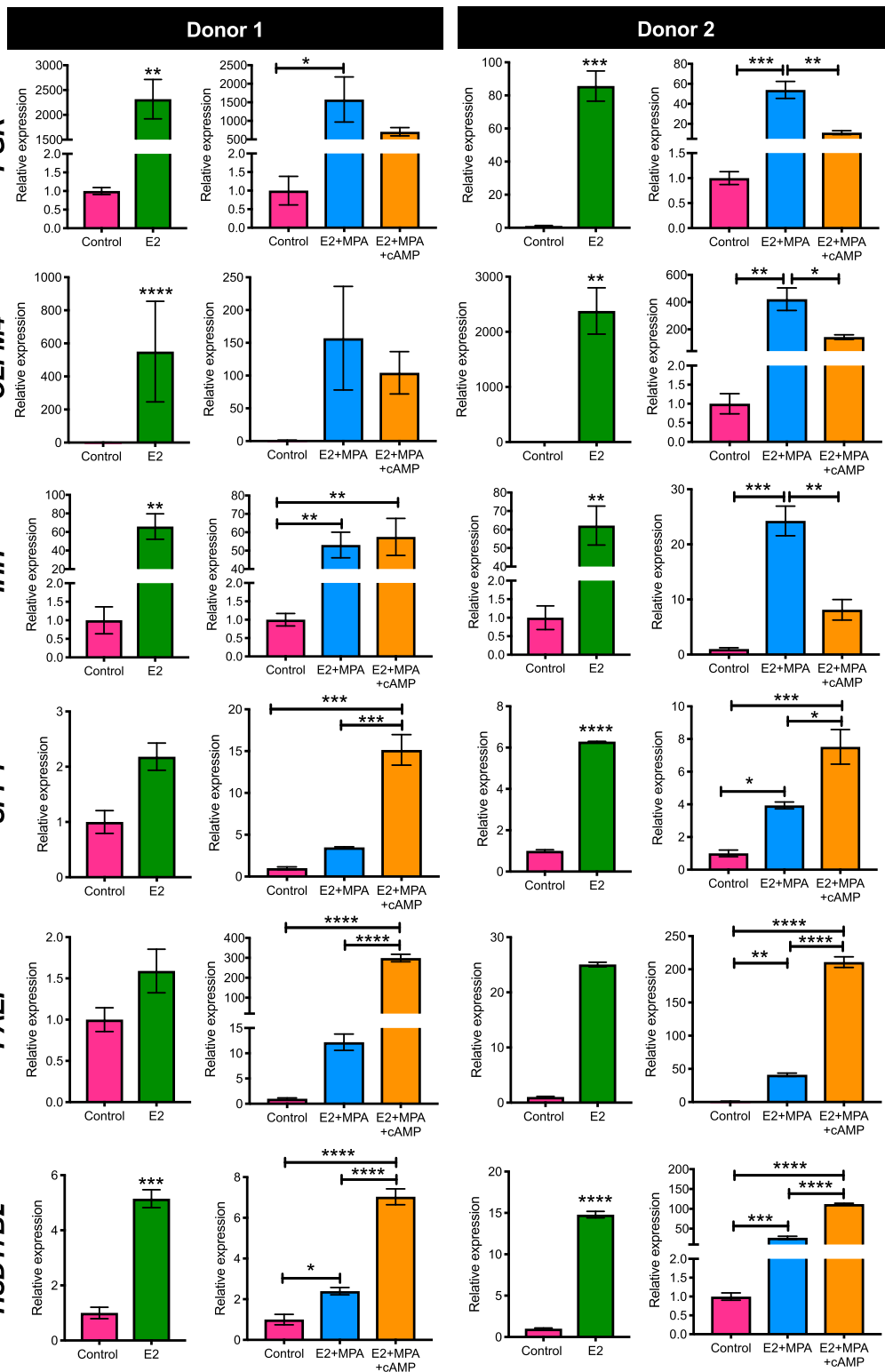


Fig. 2. Human endometrial epithelial organoids are responsive to ovarian steroid hormones. Relative *PGR*, *OLFM4*, *IHH*, *SPP1*, *PAEP*, and *HSD17B2* mRNA levels in hormone-treated organoids. Data are means \pm SEMs. * $P < 0.05$, ** $P < 0.01$, *** $P < 0.001$, **** $P < 0.0001$.

hormone. Progesterone-regulated genes were also increased in EEO by E2+MPA treatment compared to control, including *HSD17B2*, *PAEP*, and *SPP1* that aligned with qPCR results (Fig. 2). Treatment with E2+MPA decreased 476 genes in the organoids compared to control treatment including *FAM3D*,

MMP10, and *PRSS33*. E2+MPA+cAMP treatment increased 1,417 genes and decreased 609 genes compared to the control. Known P4-regulated genes, including *HSD17B2*, *LIF*, *PAEP*, and *SPP1*, were all increased by E2+MPA+cAMP treatment of EEO.

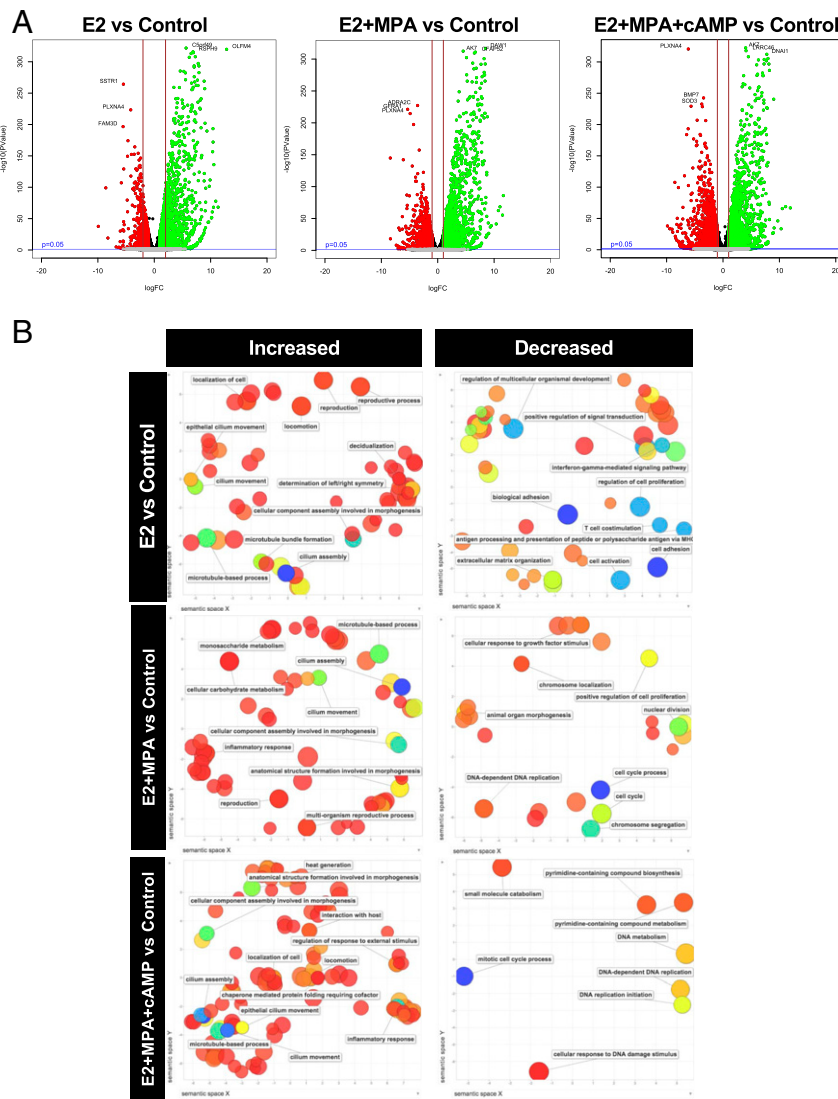


Fig. 3. Determination of hormone responsiveness in human endometrial organoids using bulk RNA-seq analysis. (A) Volcano plots of differentially expressed genes. (B) REVIGO visualization of enriched biological processes associated with genes increased or decreased in organoids by hormone treatment. Bubble size indicates the frequency of the gene ontology (GO) term identified in the analysis.

REVIGO enrichment analysis of the differentially expressed genes found that they were enriched for many different biological processes (Fig. 3B). Biological processes enriched by E2 treatment of EEO included cilium assembly and movement as well as decidualization. Genes increased by E2+MPA treatment compared to control were enriched for biological processes including the inflammatory response, while those that were decreased were enriched for DNA replication, cell proliferation, cell cycle processes, and morphogenesis. Those genes that were increased by E2+MPA+cAMP treatment compared to control were enriched again for the inflammatory response, cilia-related processes and localization, and movement of the cell. Those that were decreased were similar to the E2+MPA group in that they were enriched for DNA replication.

Single-Cell Analysis of Human EEO. Organoids were generated from Donor 2 and treated with hormones (Fig. 1A) and subjected to scRNA-seq analysis using the 10X Genomics platform. Between 4,131 and 7,384 cells were sequenced from the organoids with about 195 million reads per library. Bases with high quality ($Q > 30$) were estimated to be 98.1% of the unique molecular identities

(UMI) counts. The raw count data were filtered for cells expressing more than 200 genes and less than 20% of mitochondria transcripts. Using this filtration step, data from 3,500 to 5,990 cells were used for subsequent analyses.

Shared Nearest Neighbor and t-Distributed Stochastic Neighbor Embedding (tSNE) methods assigned cells to 12 clusters for day 6 organoids and 13 clusters for day 12 organoids (SI Appendix, Fig. S2 A and B). Gene expression of the individual clusters were analyzed to identify specific markers (Dataset S2). Known markers of different cell types were then obtained from the published literature and specific databases (19–21) and mapped to the Seurat predicted markers to assign cell types to the expression clusters (Figs. 4A and 5A). Using this approach, 5 cell types (ciliated, epithelial, proliferative, stem, and unciliated) were identified in both control and E2-treated day 6 organoids, and 6 cell types (ciliated, epithelial, secretory, proliferative, stem, and unciliated) were identified in control, E2+MPA-, and E2+MPA+cAMP-treated day 12 organoids. This analysis also revealed effects of hormone treatment on cell types in the day 6 and day 12 EEO (tables in Figs. 4A and 5A). Of note, a substantial increase in ciliated cells was noted in E2-treated day 6 EEO and E2+MPA-treated day

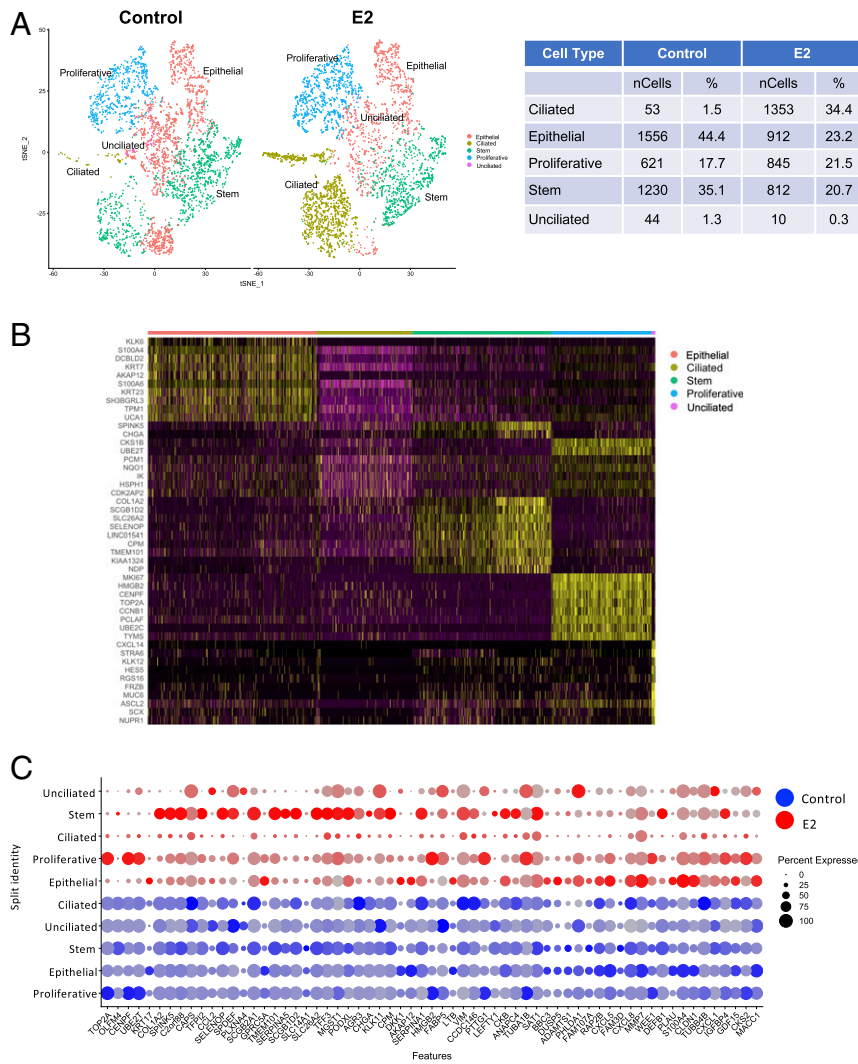


Fig. 4. Single-cell RNA-seq profiling of human endometrial organoids reveals different types of cells and responses to estrogen treatment. (A) tSNE plot revealing 5 different cell types in day 6 control and E2-treated organoids based on marker gene analysis. The number of cells (nCells) in the organoids is provided in the table as determined by marker gene analysis (*Materials and Methods*). Note the increase in proportion of ciliated cells with E2 treatment. (B) Heat map showing distinct patterns of marker gene expression among cell types in day 6 organoids. Scale represents normalized log₂ expression. (C) Dot plot representing key cell type marker gene expression and the effect of hormone treatment in each of the 5 different organoid cell types. Dot size indicates proportion of cells in cluster expressing a gene, and shading indicates the relative level of expression (low to high reflected as light to dark).

12 EEO. In day 6 EEO, the number of epithelial and stem type cells decreased with E2 treatment, whereas the other cell types (proliferative and unciliated) remained unchanged. Interestingly, the secretory cell type was found only in day 12 EEO, and the number of those cells was increased by E2+MPA treatment. The number of ciliated, epithelial, and secretory type cells increased in day 12 EEO treated with E2+MPA, whereas the number of stem and unciliated type cells decreased with E2+MPA treatment. In contrast, the number of proliferative type cells did not change with hormone treatment. Although cAMP with E2+MPA had substantial effects on organoid gene expression (Fig. 3), the number of cell types did not change with that hormone treatment.

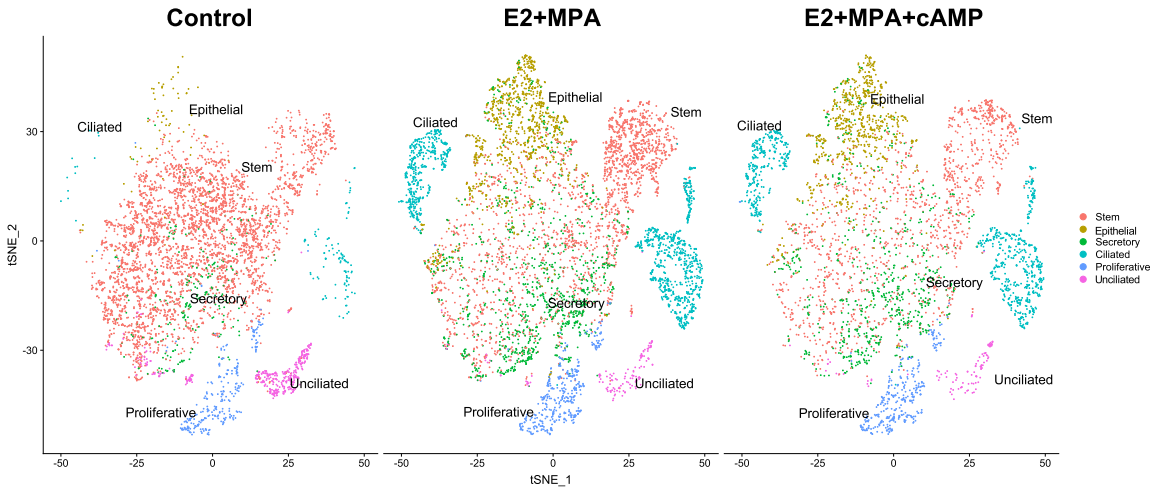
Individual cell types in the cultures displayed distinct patterns of differential gene expression in response to hormone treatment (Figs. 4 B and C and 5 B and C and Dataset S2). Changes in gene expression were most profound in the ciliated cells followed by the stem cells. This data complements the bulk RNA-seq data and allows for the determination of which cell type(s) in the organoid is responsive to steroid hormones. For instance, *OLFM4* is an E2-responsive gene that is predominantly up-regulated in the

stem and ciliated cells of the day 6 EEO. In the day 12 EEO, *PAEP* is a P4-responsive gene that is predominantly up-regulated in the ciliated, proliferative, secretory, and stem cell types by E2+MPA treatment. Differential response of cell types to hormone treatment based on gene expression cluster patterns was confirmed by mutual information analysis of coexpressed genes as well as K-means clustering of gene expression data of each cell type (22) (*SI Appendix, Fig. S3*).

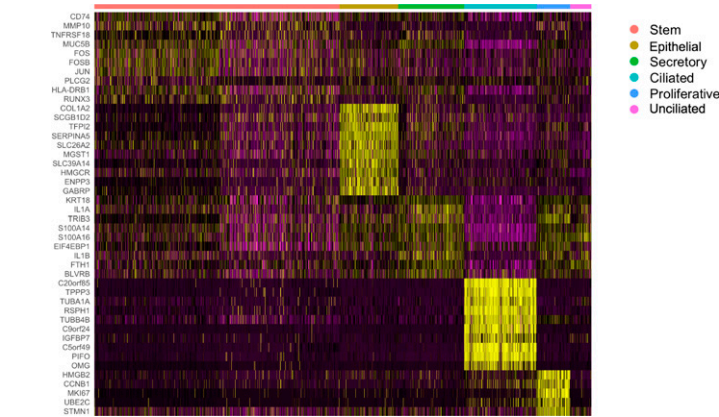
Ligand-Receptor Prediction and Analysis. Recent evidence in mice and humans supports the idea that products of the endometrial GE impacts stromal cell decidualization (17, 23–25). First, the FANTOM5 database (<http://fantom.gsc.riken.jp/5/>) (26) of ligands and receptors was used to determine ligands whose encoded genes were associated with genes increased by E2+MPA and E2+MPA+cAMP in day 12 EEO based on bulk RNA-seq analysis as described in *Materials and Methods*. Second, receptors for those ligands were determined using transcriptome data from human endometrial stromal cells (ESCs) before and after decidualization

A

Cell Type	Control		E2+MPA		E2+MPA+cAMP	
	nCells	%	nCells	%	nCells	%
Ciliated	111	2.3	1221	20.4	849	20.8
Epithelial	66	1.4	968	16.2	730	17.9
Proliferative	270	5.5	403	6.7	334	8.2
Secretory	251	5.1	1055	17.6	677	16.6
Stem	3782	77.5	2206	36.8	1388	34
Unciliated	398	8.2	137	2.3	104	2.5



B



C

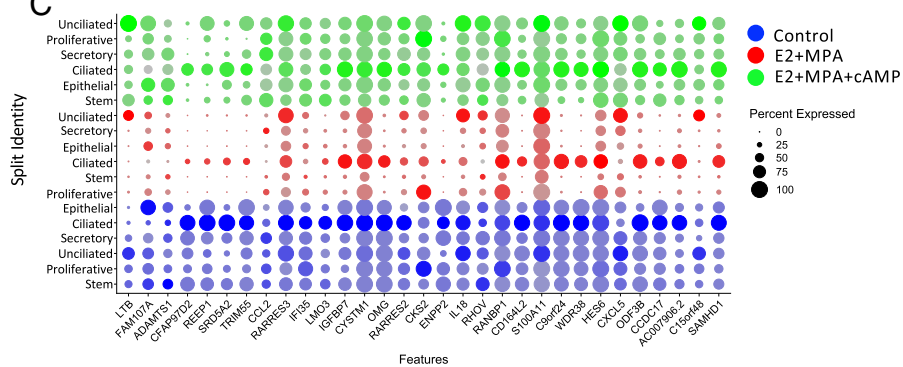


Fig. 5. Single-cell RNA-seq profiling of human endometrial organoids reveals different types of cells and responses to estrogen, progesterone, and cAMP treatment. (A) tSNE plot revealing 6 different cell types in day 12 control, E2+MPA, and E2+MPA+cAMP-treated organoids based on marker gene analysis. The number of cells (nCells) in the organoids is provided in the table as determined by marker gene analysis (*Materials and Methods*). Note the increase in proportion of ciliated and secretory cells with E2+MPA treatment. (B) Heat map showing distinct patterns of marker gene expression among cell types in day 12 organoids. Scale represents normalized \log_2 expression. (C) Dot plot representing key cell type marker gene expression and the effect of hormone treatment in each of the 6 different organoid cell types. Dot size indicates proportion of cells in cluster expressing a gene, and shading indicates the relative level of expression (low to high reflected as light to dark).

in vitro (National Center for Biotechnology Information GEO accession no. GSE112362) (27).

As expected, a large number of ligands were expressed by the control and hormone-treated EEO with corresponding receptors expressed in the undecidualized and decidualized ESCs. Next, differentially expressed receptors were determined in the ESCs and decidualized ESCs based on the RNA-seq analysis. Then, ligands from the control organoids were determined as well as ligands that are differentially expressed between hormone-treated and control organoids (Fig. 6 and Dataset S3). For example, the ligands CALM3 (calmodulin 3), FN1 (fibronectin 1), TIMP2 (TIMP metalloproteinase inhibitor 2), and TNC (tenascin C) were found in day 12 control EEO in levels significantly different from those treated with either E2+MPA or E2+MPA+cAMP. Several receptors, mostly integrins, were found to be differentially expressed in the undecidualized as compared to decidualized stromal cells. The treatment of organoids with E2+MPA increased the expression of COL1A2 (collagen type I alpha 2) and JAG1, whereas the addition of cAMP resulted in differential regulation of IL1RN (Interleukin 1 Receptor Antagonist), SPPI1, and TGM2.

Second, an integrative analysis using the single-cell RNA-seq data were performed to determine potential interactions between individual cell types in the EEO with in vitro decidualized ESCs and their progenitors in vitro. This analysis predicted a large number of reciprocal ligand–receptor interactions occur in a cell-specific manner (SI Appendix, Figs. S4–S6 and Dataset S3). Collectively, these analyses support the idea that endometrial epithelia, particularly the GE, produces factors that communicate with decidualizing stromal cells and other cell types, such as the invading trophoblast as well as immune cells, during the perimplantation period of pregnancy.

Discussion

This study highlights that human EEO are comprised of the major epithelial cell types that are normally found in the endometrium including both LE and GE. The FOXA2 transcription factor is expressed specifically in the GE of all studied mammalian uteri (17, 6, 28) and regulates GE differentiation and function (23, 24, 29, 30). The EEO generated in this and other studies (10–13) contained both FOXA2⁺ and FOXA2⁻ cells, signifying they are a mixture of LE and GE. Organoids established from other human tissues such as prostate, intestine, lung, kidney, and oviducts or Fallopian tubes are also comprised of different epithelial cell types at different stages of differentiation, highlighting their similarity to those in vivo (31–35). Here, analysis using scRNA-seq found that day 6 control and E2-treated EEOs were made up of 5 cell types, i.e., proliferative, epithelial, ciliated, unciliated, and stem. The day 12 EEOs were made up of 6 cell types, including the same 5 as day 6, and also a secretory cell population. Previous EEO studies revealed gene expression of markers related to epithelial, mucosal secretory, and epithelial progenitor cells as well as electron microscopy and gene expression analyses showing evidence of ciliated cells (10–12). In women, the endometrial epithelium is morphologically differentiated into the LE and GE, both are either ciliated or

unciliated, and the proportion of those cells changes across the menstrual cycle stage (36, 37). During menstruation, the functional layer of the endometrium is shed, which is followed by reepithelialization, regeneration, and cellular proliferation during the proliferative phase. Differentiation and secretory transformation of the endometrial glands occurs during the subsequent secretory phase and, if pregnancy does not occur, the entire process repeats, typically in a 28-d cycle. As such, to recapitulate the hormonally controlled in vivo environment, EEO should also be comprised of proliferating, secretory, and putative stem cell populations as determined by single-cell RNA-seq analysis in the present study.

The ability of the organoids to be maintained in culture long-term and to maintain proliferative capacity suggests that a population of epithelial stem cells is present. Previous EEO studies established their clonogenicity (10, 11). Clonogenic activity of human endometrial epithelial cells was first shown when in culture, single epithelial cells in culture were able to form a colony at low densities (38). While this was possible, the number of cells able to produce these colonies was small as were the colonies themselves. Although extensive efforts have been subsequently made to identify markers of endometrial epithelial stem/progenitor cells, such as CDH1, SSEA-1, and LGR5 (39–42), the identity of these clonogenic progenitors as legitimate stem cells remains largely unknown. Turco et al. (11) found that endometrial epithelial organoids formed from SSEA-1–negative cells. Those published endometrial epithelial stem cell markers were identified in the bulk RNA-seq data from the EEO here, but not in the stem cell cluster determined by scRNA-seq analysis. However, the cell type designations of the scRNA-seq analysis relied on a dataset of stem cell marker genes curated from tissues other than the endometrium. Nevertheless, analysis of EEO should provide significant insights into endometrial epithelial stem cell dynamics that occur in the developing and adult human uterus.

Estrogen treatment instigated changes in organoid gene and protein expression as well as cell composition that mimics the in vivo endometrium during the proliferative phase of the menstrual cycle. Treatment with E2 increased the number of ESR1- and PGR-positive cells. This replicates in vivo changes in the proliferative phase of the menstrual cycle when many GE cells in the functionalis and basalis layers of the endometrium express ESR1 and PGR (43–45). Furthermore, others have shown a positive correlation between plasma E2 levels and the PGR content in uterine tissues and primary endometrial cells treated with E2 have increased expression of PGR (46, 47). Treatment with E2 also significantly amplified *OLFM4*, and this was the most significantly increased gene in the bulk RNA-seq analysis. This reflects in vivo and previous cell culture experiments where *OLFM4* expression is highest during the proliferative phase and E2 treatment of endometrial explants stimulates *OLFM4* expression (48). Stimulation with E2 also increased *IHH* expression in the absence and presence of MPA in the EEO. In the mouse uterus, *Ihh* is a mediator of P4 action and is expressed in the murine epithelium under the control of P4 (49). Immunohistochemical studies of the human endometrium found that *IHH* is increased in secretory phase glands and stroma as compared to

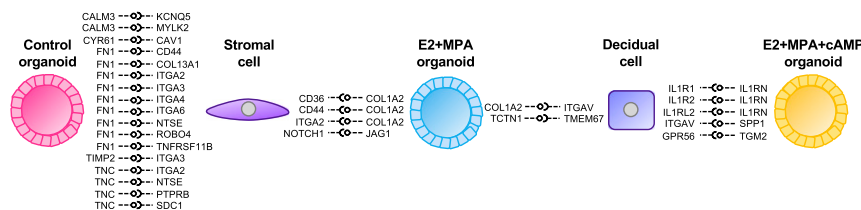


Fig. 6. Ligand receptor analysis of EEOs and stromal cells. Integrative analysis of bulk and single-cell RNA-seq data for identification of consensus ligands expressed in day 12 organoids whose receptors are expressed in either stromal cells or decidual cells.

The development of EEOs cultured in a defined medium (10, 11) has allowed for the expansion and cryopreservation of endometrial epithelial cells, which was previously difficult to achieve. These EEOs are hormone-responsive and express known markers of differentiation under P4 treatment, reflective of the secretory phase of the menstrual cycle when the endometrium is receptive to embryo implantation in women. A comprehensive analysis of EEO was performed under the influence of both E2 and P4 in an unbiased approach using both bulk RNA-seq and single-cell RNA-seq technologies. Importantly, the organoids express genes similar to that of uterine glands and consist of the different epithelial cell types found in the *in vivo* environment. These analyses provide a crucial contribution to our understanding of uterine glands and allow for the further development of this model to incorporate other endometrial cell types to better understand pregnancy establishment and complications in women. The EEOs can also be utilized as a platform to discover genes and regulatory mechanisms that impact endometrial regeneration and differentiation and how this influences early pregnancy establishment. The cryopreservation of organoids derived from different donors with normal endometrium and endometrial pathologies allows for comparative studies into the specific mechanisms that may drive endometrial dysfunction as well as the responsiveness of these cells to potential treatments that target pregnancy complications such as preeclampsia, pregnancy loss, and infertility.

Materials and Methods

Establishment, Maintenance, and Cryopreservation of Human Uterine EEOs. All experiments involving human subjects were approved by the Institutional Review Board of the University of Missouri, and written informed consent was obtained from each donor. Donor 1 was 35 y old, having a nonfunctional ovarian cyst removed, and cycle day 27 (late secretory phase). Donor 2 was 28 y old, having a vaginal cyst excised, and cycle day 9 (proliferative phase). Both were Caucasian.

Upon collection, endometrial tissue biopsies were immediately placed in Dulbecco's modified eagle medium: nutrient mixture F-12 medium (DMEM/F12) (Gibco, 11320-033) supplemented with 10% fetal bovine serum (FBS) (Sigma, F0926) and 1% antibiotic-antimycotic (Anti-Anti, Gibco, 15240-062) at 4 °C. Endometrial tissues were washed with DMEM/F12 medium supplemented with 1% antibiotic-antimycotic for 20 min at 37 °C with gentle agitation to remove blood and debris. Tissues were transferred to a Petri dish and finely minced with scissors. Minced tissue was placed in 20 mL of enzymatic digestion solution (DMEM/F12 supplemented with 1% antibiotic-antimycotic, 0.4 mg/mL Collagenase V [Sigma, C-9263], 1.25 U/mL dispase II [Sigma, D4693]) and incubated at 37 °C with agitation. The extent of digestion was checked after 20 min and, depending on the amount of tissue, total digestion time was between 40 and 50 min. Once digested, 20 mL of neutralizing medium (DMEM/F12 supplemented with 1% anti-anti and 10% FBS), was added to the tissue/digestion solution to halt further digestion. The Falcon tube containing the digested tissue was swirled firmly and left to stand for 2 min to allow any undigested tissue fragments to settle at the bottom of the Falcon tube. The supernatant was passed through 1 or more 100- μ m cell strainers and rinsed with DMEM/F12 supplemented with 1% anti-anti medium. The 100- μ m strainer was inverted over a Petri dish, and the glandular fragments/epithelial cells were forcefully backwashed, transferred to a Falcon tube, and pelleted by centrifugation. The supernatant was removed and the glandular fragments resuspended in 1 mL of advanced DMEM/F12 medium (Gibco, 12634010). The tissue/cell suspension was pipetted up and down repeatedly to separate glandular fragments and pelleted by centrifugation. The supernatant was removed and tube with pellet placed on ice for 2–3 min. The pellet was loosened by flicking the tube and cells/glandular fragments were resuspended in Matrigel (Corning, 536231) at a volume according to volume recommended by Turco et al. (11) and placed on ice. Twenty-microliter droplets of the Matrigel cell suspension were added to a 48-well plate (1 droplet per well) and incubated at 37 °C for 15 min. Organoid medium (250 μ L) was overlaid in each well. The organoids formed within 3–4 d and were passaged according to growth and confluency within the Matrigel.

To passage the organoids, a 1-mL pipette was used to scrape the Matrigel droplets from the well of the cell culture plate so that they detached into the organoid medium. The Matrigel/organoids and medium were transferred to a Falcon tube and centrifuged for 10 min at 4 °C. The medium/supernatant was removed, replaced by 1 mL of Advanced DMEM/F12 (Gibco, 12634010),

and pipetted up and down to dissociate the pellet. Another 1 mL of Advanced DMEM/F12 medium was added to the cell suspension; the suspension was mixed by pipetting and centrifuged for 10 min at 4 °C. The supernatant was removed and the pellet placed on ice for 3 min. The cells were then resuspended in Matrigel, and 20- μ L droplets of Matrigel/cells were plated onto a 12-well cell culture plate (3–4 droplets per well), followed by incubation at 37 °C for 15 min to allow the droplets to set. Seven hundred microliters per well of organoid medium was overlaid in each well.

Cryopreservation of organoids was achieved by first passaging the organoids as mentioned previously and following the second centrifugation and removal of supernatant, the organoids were resuspended in 1 mL of freezing medium consisting of 10% DMSO in FBS and placed in cryovials at –80 °C overnight. Organoids were then transferred to liquid nitrogen for long-term storage. To thaw, organoids were removed from liquid nitrogen and thawed by pipetting 500- μ L aliquots of warmed organoid medium added serially into the cryovial. The thawed vial contents were then transferred to a 15-mL Falcon tube. This was repeated as many times as necessary until all contents of the cryovial were thawed and freezing medium was diluted. Following centrifugation for 10 min, the supernatant was removed and pellet resuspended in 1 mL of organoid medium by gently pipetting up and down. The cell suspension was again centrifuged for 10 min, supernatant was removed, and the pellet resuspended in Matrigel and placed on ice for 3 min. Twenty-microliter droplets of Matrigel were placed in a 48-well cell culture plate and incubated for 15 min at 37 °C. Organoid medium supplemented with 10 μ M Y-27632 was overlaid in each well and used for the first 3 media changes. Following this, normal organoid medium was used for continued culture.

Hormone Treatment of Organoids. To examine the hormone responsiveness of organoids following passaging, 10,000 cells per Matrigel droplet were plated in 12-well plates (3 droplets per well) and allowed to establish into organoids over 4 d in organoid medium. Organoids were then treated with either 10 nM estradiol (E2, Sigma, E1024) or vehicle as a control (100% ethanol) for 2 d. Following this, organoids were treated with either 10 nM E2 and 1 μ M MPA (Sigma, PHR1589) (E2+MPA), 10 nM E2, 1 μ M MPA, and 1 μ M cAMP (2'-O-dibutyryl adenosine 3', 5'-cyclic monophosphate sodium salt; Sigma, D0627) (E2+MPA+cAMP) for a further 6 d. Each treatment was performed in triplicate wells with a fourth well for each treatment used for histology purposes. Organoids derived from 2 individual donors were used.

Organoid Dissociation for Single-Cell Analysis. Hormone treatment of organoids was performed as described above. Following treatment, a 1-mL pipette was used to scrape the Matrigel droplets from the well of the cell culture plate so that they detached into the organoid medium. The Matrigel/organoids and medium were transferred to a Falcon tube, the volume increased to 10 mL using serum-free DMEM/F12 supplemented with antimycotic-antibiotic, and the mixture was placed on ice for 5 min. The organoid suspension was centrifuged for 10 min at 4 °C, the supernatant removed, and the pellet resuspended in 10-mL serum-free DMEM/F12 supplemented with antimycotic-antibiotic. Following an additional centrifugation, the supernatant was removed and pellet resuspended in 0.05% trypsin EDTA to dissociate organoids. This mixture was incubated for 40 min at 37 °C with resuspension via pipetting 10 min to create a single-cell suspension. Suspension volume was increased to 10 mL with serum-free DMEM/F12 supplemented with antimycotic-antibiotic and the mixture centrifuged. Pelleted cells were resuspended in serum-free DMEM/F12 supplemented with antimycotic-antibiotic and 1 mg/mL DNase I and incubated for 5 min at 37 °C. An equal volume of serum-free DMEM/F12 supplemented with antimycotic-antibiotic was added to the cell suspension, and the suspension mixed and centrifuged. The supernatant was removed, and the pellet was resuspended in 1-mL PBS containing 0.04% BSA. This mixture was passed through a 40- μ m cell strainer. Another 1 mL of PBS containing 0.04% bovine serum albumin (BSA) was passed through the cell strainer. The cells were counted and viability assessed.

scRNA-Seq and Data Analysis. Droplet generation of single cells was performed using a 10X Chromium system with a target cell count of 4,000 per sample. Single-cell RNA-seq libraries were prepared using 10X Chromium technology using the manufacturer's protocol at the University of Missouri DNA Core facility. Libraries were sequenced on an Illumina NextSeq with a target reads per cell of 25,000. The BCL (base call) files generated from Illumina sequencing were processed by Cell Ranger (v. 3.0.1), the proprietary pipeline for single-cell sequence analysis by 10X Genomics. The "mkfastq" function of Cell Ranger was used to demultiplex the raw base call (BCL) files into FASTQ files, which were then used to map to the human reference genome GRCh38 using STAR aligner. The "count" function of Cell Ranger was used to count barcodes, UMI, perform background filtration based on

UMI vs. barcode counts, and generate feature-barcode matrices based on the barcodes used in the sequencing libraries. The Cell Ranger pipeline also generated the summary statistics of cell counts, read counts, and mapping information relative to the genome.

The R package “Seurat” was used to analyze the expression count data generated by Cell Ranger. The count data were read using “Read10x” function of Seurat that was then used to create Seurat object for each sample. Cells were filtered with lower gene expression (nfeature < 200) and a higher percentage (>20) of mitochondrial origin as described (19). The variable genes in the normalized filtered data were detected by using the “FindVariableFeatures” function of Seurat for each sample separately. In order to compare the hormone treatment sample with the control sample, we integrated day 6 control and E2 treated data by finding integration anchors using the first 20 dimensions of data variation. The anchors were then used to integrate expression data of control and treatment samples using the “IntegrateData” function of Seurat. A similar approach was used to integrate data of the control and the 2 treatments (E2+MPA and E2+MPA+cAMP). The scaled integrated data were then used to determine the principal components of expression variation with the nonlinear dimensional reduction method of UMAP (Uniform Manifold Approximation and Projection) and tSNE methods implemented in Seurat. Marker genes for individual clusters were predicted using the “FindAllMarkers” function and the list of the predicted markers were compared with known cell type markers (19–21) in order to assign cell types to different expression clusters. The heatmaps, dot plots, and violin plots were generated using plotting functions of Seurat. The mutual information (MI) plot was generated by

calculating pairwise MI matrix based on mean expression variation among the cell types and plotting by R package “circlize.”

For the single-cell sequencing analysis, the K-means cluster tree of gene expression variation between control and hormone treatment samples were conducted as follows. First, the expression data were extracted in matrix form from the RNA “count” slot Seurat object by using the GetAssayData function. If a gene had the sum of read counts across the cells less than 10, it was removed from the K-means clustering. The clustering was performed with different K values (1–5) with 100 iterations and 10 random seeds. The clusters identified from control and treated cells using this method were used for cluster tree analysis plotting was done with the R package “clustree.” The method of cluster tree analysis was based on descriptions in Zappia and Oshlack (22). All statistical analyses were conducted in R.

Immunofluorescence Analysis, Real-Time qPCR, Bulk RNA-Seq Analysis, Ligand-Receptor Analysis, and Statistical Analyses. Full details can be found in *SI Appendix, SI Materials and Methods*.

Data Availability. RNA-seq data reported in this paper is deposited in the Gene Expression Omnibus (GEO) database (accession no. GSE136795).

ACKNOWLEDGMENTS. We thank members of the T.E.S. laboratory for helpful discussions. The work was supported by NIH Grant R01 HD096266 (to T.E.S.) and the University of Missouri System Research and Creative Works Strategic Research Investment Program.

1. O. D. Genbacev *et al.*, Trophoblast L-selectin-mediated adhesion at the maternal-fetal interface. *Science* **299**, 405–408 (2003).
2. E. R. Norwitz, D. J. Schust, S. J. Fisher, Implantation and the survival of early pregnancy. *N. Engl. J. Med.* **345**, 1400–1408 (2001).
3. N. M. Falkiner, A description of a human ovum fifteen days old with special reference to the vascular arrangements and to the morphology of the trophoblast. *J. Obstet. Gynaecol. Br. Emp.* **39**, 471–506 (1932).
4. B. Gellersen, J. J. Brosens, Cyclic decidualization of the human endometrium in reproductive health and failure. *Endocr. Rev.* **35**, 851–905 (2014).
5. T. E. Spencer, Biological roles of uterine glands in pregnancy. *Semin. Reprod. Med.* **32**, 346–357 (2014).
6. A. M. Kelleher, F. J. DeMayo, T. E. Spencer, Uterine glands: Developmental biology and functional roles in pregnancy. *Endocr. Rev.* **40**, 1424–1445 (2019).
7. A. R. Chavan, B. A. Bhullar, G. P. Wagner, What was the ancestral function of decidual stromal cells? A model for the evolution of eutherian pregnancy. *Placenta* **40**, 40–51 (2016).
8. T. Garrido-Gomez *et al.*, Severe pre-eclampsia is associated with alterations in cytotrophoblasts of the smooth chorion. *Development* **144**, 767–777 (2017).
9. T. Garrido-Gomez *et al.*, Defective decidualization during and after severe pre-eclampsia reveals a possible maternal contribution to the etiology. *Proc. Natl. Acad. Sci. U.S.A.* **114**, E8468–E8477 (2017).
10. M. Boretto *et al.*, Development of organoids from mouse and human endometrium showing endometrial epithelium physiology and long-term expandability. *Development* **144**, 1775–1786 (2017).
11. M. Y. Turco *et al.*, Long-term, hormone-responsive organoid cultures of human endometrium in a chemically defined medium. *Nat. Cell Biol.* **19**, 568–577 (2017).
12. S. Haider *et al.*, Oestrogen signalling drives clonogenesis in human endometrial organoids. *Endocrinology* **160**, 2282–2297 (2019).
13. M. Boretto *et al.*, Patient-derived organoids from endometrial disease capture clinical heterogeneity and are amenable to drug screening. *Nat. Cell Biol.* **21**, 1041–1051 (2019).
14. A. Roy, M. M. Matzuk, Reproductive tract function and dysfunction in women. *Nat. Rev. Endocrinol.* **7**, 517–525 (2011).
15. L. Aghajanova, A. E. Hamilton, L. C. Giudice, Uterine receptivity to human embryonic implantation: Histology, biomarkers, and transcriptomics. *Semin. Cell Dev. Biol.* **19**, 204–211 (2008).
16. B. Gellersen, J. Brosens, Cyclic AMP and progesterone receptor cross-talk in human endometrium: A decidualizing affair. *J. Endocrinol.* **178**, 357–372 (2003).
17. A. M. Kelleher *et al.*, Integrative analysis of the forkhead box A2 (FOXA2) cistrome for the human endometrium. *FASEB J.* **33**, 8543–8554 (2019).
18. B. A. Lessey *et al.*, Immunohistochemical analysis of human uterine estrogen and progesterone receptors throughout the menstrual cycle. *J. Clin. Endocrinol. Metab.* **67**, 334–340 (1988).
19. M. L. Mucenski, R. Mahoney, M. Adam, A. S. Potter, S. S. Potter, Single cell RNA-seq study of wild type and Hox9,10,11 mutant developing uterus. *Sci. Rep.* **9**, 4557 (2019).
20. X. Zhang *et al.*, CellMarker: A manually curated resource of cell markers in human and mouse. *Nucleic Acids Res.* **47**, D721–D728 (2019).
21. A. Hatano *et al.*, CELLVEDIA: A repository for human cell information for cell studies and differentiation analyses. *Database (Oxford)* **2011**, bar046 (2011).
22. L. Zappia, A. Oshlack, Clustering trees: A visualization for evaluating clusterings at multiple resolutions. *Gigascience* **7**, giy083 (2018).
23. A. M. Kelleher, J. Milano-Foster, S. K. Behura, T. E. Spencer, Uterine glands coordinate on-time embryo implantation and impact endometrial decidualization for pregnancy success. *Nat. Commun.* **9**, 2435 (2018).
24. A. M. Kelleher *et al.*, Forkhead box a2 (FOXA2) is essential for uterine function and fertility. *Proc. Natl. Acad. Sci. U.S.A.* **114**, E1018–E1026 (2017).
25. L. L. Shuya *et al.*, Leukemia inhibitory factor enhances endometrial stromal cell decidualization in humans and mice. *PLoS One* **6**, e25288 (2011).
26. J. A. Ramiłowski *et al.*, A draft network of ligand-receptor-mediated multicellular signalling in human. *Nat. Commun.* **6**, 7866 (2015). Erratum in: *Nat. Commun.* **7**, 10706 (2016).
27. R. Kommagani *et al.*, The promyelocytic leukemia zinc finger transcription factor is critical for human endometrial stromal cell decidualization. *PLoS Genet.* **12**, e1005937 (2016).
28. T. E. Spencer, A. M. Kelleher, F. F. Bartol, Development and function of uterine glands in domestic animals. *Annu. Rev. Anim. Biosci.* **7**, 125–147 (2019).
29. A. M. Kelleher, G. W. Burns, S. Behura, G. Wu, T. E. Spencer, Uterine glands impact uterine receptivity, luminal fluid homeostasis and blastocyst implantation. *Sci. Rep.* **6**, 38078 (2016).
30. J. W. Jeong *et al.*, Foxa2 is essential for mouse endometrial gland development and fertility. *Biol. Reprod.* **83**, 396–403 (2010).
31. T. McCray, D. Moline, B. Baumann, D. J. Vander Griend, L. Nonn, Single-cell RNA-Seq analysis identifies a putative epithelial stem cell population in human primary prostate cells in monolayer and organoid culture conditions. *Am. J. Clin. Exp. Urol.* **7**, 123–138 (2019).
32. N. Sachs *et al.*, Long-term expanding human airway organoids for disease modeling. *EMBO J.* **38**, e100300 (2019).
33. A. N. Combes, L. Zappia, P. X. Er, A. Oshlack, M. H. Little, Single-cell analysis reveals congruence between kidney organoids and human fetal kidney. *Genome Med.* **11**, 3 (2019).
34. M. Kessler *et al.*, The Notch and Wnt pathways regulate stemness and differentiation in human fallopian tube organoids. *Nat. Commun.* **6**, 8989 (2015).
35. T. Sato *et al.*, Long-term expansion of epithelial organoids from human colon, adenoma, adenocarcinoma, and Barrett’s epithelium. *Gastroenterology* **141**, 1762–1772 (2011).
36. A. Ferenczy, R. M. Richart, F. J. Agate, Jr, M. L. Purkerson, E. W. Dempsey, Scanning electron microscopy of the human endometrial surface epithelium. *Fertil. Steril.* **23**, 515–521 (1972).
37. E. F. Schueller, Ciliated epithelia of the human uterine mucosa. *Obstet. Gynecol.* **31**, 215–223 (1968).
38. R. W. S. Chan, K. E. Schwab, C. E. Gargett, Clonogenicity of human endometrial epithelial and stromal cells. *Biol. Reprod.* **70**, 1738–1750 (2004).
39. F. L. Cousins, D. F. O, C. E. Gargett, Endometrial stem/progenitor cells and their role in the pathogenesis of endometriosis. *Best Pract. Res. Clin. Obstet. Gynaecol.* **50**, 27–38 (2018).
40. H. P. T. Nguyen *et al.*, N-cadherin identifies human endometrial epithelial progenitor cells by in vitro stem cell assays. *Hum. Reprod.* **32**, 2254–2268 (2017).
41. C. E. Gargett, K. E. Schwab, J. A. Deane, Endometrial stem/progenitor cells: The first 10 years. *Hum. Reprod. Update* **22**, 137–163 (2016).
42. N. Tempest, A. M. Baker, N. A. Wright, D. K. Hapangama, Does human endometrial LGR5 gene expression suggest the existence of another hormonally regulated epithelial stem cell niche? *Hum. Reprod.* **33**, 1052–1062 (2018).

